PROCEEDINGS, 44th Workshop on Geothermal Reservoir Engineering
Stanford University, Stanford, California, February 11-13, 2019
SGP-TR-214

# Induced Earthquakes by Hot Dry Rock Power Generation: Influence of Injection Energy and Underground Structure

Tamaki Ishikawa and Koichi Yamada

Yonbancho 5-3 Chiyoda-ku Tokyo Japan

ishikawa@jst-lcs.jp

**Keywords:** water injection energy, earthquake energy, hydraulic fracturing, natural fracture, hot dry rock

## ABSTRACT

When performing hydraulic fracturing to create an artificial reservoir for hot dry rock power generation, it is important to suppress induced earthquakes. However, the relationship between the magnitude of the induced earthquake and the hydraulic fracturing conditions has not been clarified. We investigated the relationship between water injection energy and induced earthquake energy, and obtained useful information for the design of hot dry rock power generation sites.

Data from six sites in Japan, Australia, Switzerland, and the United States were used for our investigation. For reference, we also investigated sites performing wastewater injection and carbon capture and sequestration. Water injection energy was calculated as the product of well head pressure, flow rate, and time, and induced earthquake energy was calculated using the Gutenberg-Richter formula. As a result, it was found that the ratio of total induced earthquake energy to water injection energy varies greatly from 0.0001% to 6.4%.

Induced earthquake energy is considered to be dependent on underground structures. We examined reported values of natural fracture density in underground structures, and clarified that natural fracture density and maximum magnitude of induced earthquakes were closely related at the six sites studied. Furthermore, we showed that total induced earthquake energy can be expressed using an empirical formula that is a function of water injection energy and natural fracture density. The methodology described in this paper, based on water injection energy and earthquake energy, should prove useful for selecting candidate sites for hot dry rock power generation and for setting hydraulic fracturing conditions in the field.

## 1. INTRODUCTION

Hot dry rock geothermal energy is a potentially important energy source for commercial power generation. To harness hot dry rock energy, it is necessary to create artificial reservoirs in the underground hot rock mass, usually by hydraulic fracturing.. When such fracturing is applied to create reservoirs with adequate size and permeability, there is a risk of inducing earthquakes. It is important to suppress these earthquakes induced by hydraulic fracturing , but there have been few studies that address the quantitative relationship between hydraulic fracturing conditions and induced earthquakes, although some studies have been conducted as part of hydraulic fracturing (Boroumand and Eaton, 2012) (Kaieda et al., 2010). In this paper we focus on energy balance to quantitatively understand induced earthquake activity.

Water injection energy is calculated by the product of the well head pressure, flow rate, and operation time, and induced earthquake energy can be quantified using the Gutenberg-Richter formula (Gutenberg and Richter, 1956) using published earthquake magnitudes. This study focuses on six sites with injection depths in the range 1000-5000 m. These sites were Hijiori and Ogachi (Japan), Newberry (Oregon, USA), Soultz (France), Basel (Switzerland) and Cooper Basin (Australia), We attempt to clarify the relationship of induced earthquake energy to water injection energy for each of these sites. As a reference, we also investigate the effects of wastewater injection at Youngstown (Ohio, USA) and carbon capture and sequestration activities (CCS) at Tomakomai (Japan).

The magnitude of an induced earthquake depends on water injection conditions and underground structure. Using literature data on natural fracture density in underground structures, we examine the relationship between maximum magnitude of induced earthquake and natural fracture density. Furthermore, we derive an empirical formula for total induced earthquake energy as a function of water injection energy and natural fracture density.

## 2. WATER INJECTION ENERGY AND INDUCED EARTHQUAKE ENERGY

We calculated water injection energy $E_i$ (J) of hydraulic fracturing by the product of well head pressure P(Pa), flow rate F($m^3$/s), and time t(s), that is,

$$E_i = PFt \qquad (1)$$

(Yamada et al., 2017). Figure 1 shows well head pressures and flow rates of hydraulic fracturing fluids collected during tests conducted in Hijiori in 1992 (Kaieda et al., 2010). Water injection energy was calculated to be 47 GJ.

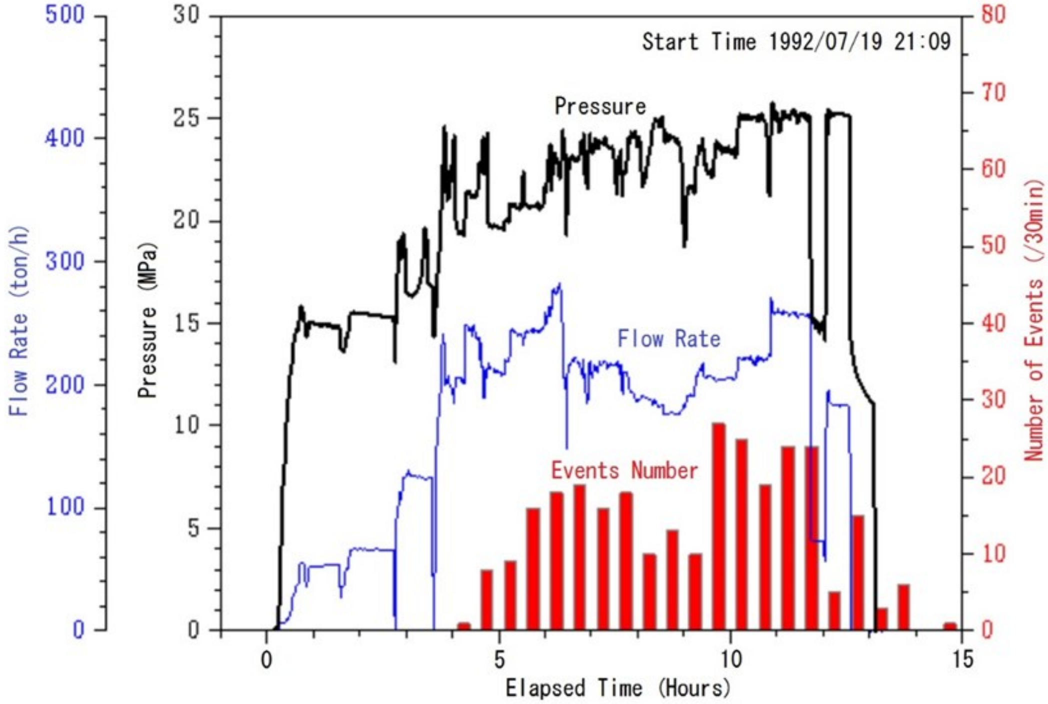


**Figure 1: Hydraulic fracturing data in Hijiori in 1992.**

The induced earthquake energy $E_s$ (J) can be calculated using the published earthquake magnitude M, using the equation of Gutenberg and Richter (1956):

$$\mathrm{Log}(E_s) = 1.5M + 4.8 \quad (2)$$

### 2.1 Hijiori

The maximum magnitude of an induced earthquake in Hijiori in 1992 was 0.3, and smaller magnitudes of other induced earthquakes were not reported (Kaieda et al., 2010). The induced earthquake energy 0.2 MJ of magnitude 0.3 was taken as the total induced earthquake energy.

### 2.2 Ogachi

The maximum magnitude of an induced earthquake in Ogachi in 1991 was measured at 2.0, while the magnitudes of other induced earthquakes were negligible (Kaieda et al., 2010). The induced earthquake energy 0.06 GJ of magnitude 2.0 was taken as the total induced earthquake energy.

### 2.3 Newberry

A total of 383 induced earthquakes of magnitude 0.1 to 2.6 were recorded at Newberry in 2012. The total induced earthquake energy was 4.1 GJ.

### 2.4 Soultz

More than 7,000 induced earthquakes were recorded in Soultz in 2000 (Schoenball and Kohl, 2013). Of these, 220 induced earthquakes had magnitudes between 1.5 and 2.6, with a total calculated energy of 6.8 GJ.

### 2.5 Basel

The Basel area experienced more than 3,500 induced earthquakes in 2006 (Häring et al., 2008); 244 induced earthquakes were of magnitude 0.5 to 3.4 and totaled 12.5 GJ in energy.

### 2.6 Cooper Basin

Eleven induced earthquakes with magnitude 2.5 to 3.7 were reported in Cooper Basin in 2003, and the total induced earthquake energy was 55.9 GJ.

### 2.7 Tomakomai

Injection started in April 2016 at the Tomakomai CCS site and is still ongoing. The depth of the reservoir is about 1000 m. Three micro-earthquakes with magnitudes 0.31 to 0. 52 were observed on August 2017, and the depth of the epicenter was estimated to be 7,400 to 7,700 m (Japan CCS Co. Ltd., 2018). The total energy of these induced earthquakes was 0.82 MJ.

### 2.8 Youngstown

Wastewater injection at Youngstown began in December 2010 (Kim, 2013), and 129 induced earthquakes of magnitude 0.1 to 3.8 have been reported to date. Total induced earthquake energy was 34.6 GJ.

Water injection energy $E_i$ and total induced earthquake energy $E_{st}$ at each of the eight sites are shown in Table 1.

**Table.1**

| Site (Country) | Water injection duration (days) | Water injection energy $E_i$ (GJ) | Total induced earthquake energy $E_{st}$ (GJ) | $E_{st}$ / $E_i$ (%) |
|---|---|---|---|---|
| Hijiori (Japan) | 1 | 47 | 0.0002 | 0.0004 |
| Ogachi (japan) | 12 | 189 | 0.06 | 0.03 |
| Newberry (USA) | 53 | 347 | 4.1 | 1.2 |
| Soultz (France) | 7 | 300 | 6.8 | 2.3 |
| Basel (Switzerland) | 7 | 288 | 12.5 | 4.3 |
| Cooper Basin (Australia) | 11 | 879 | 55.9 | 6.4 |
| Tomakomai (Japan) | 479 | 755 | 0.00082 | 0.0001 |
| Youngstown (USA) | 365 | 1193 | 34.6 | 2.9 |

The size of the reservoir for the Tomakomai CCS project is 3,800 m in width, 4,100 m in length, and 100 m in thickness, and the reservoir volume is calculated as 312,000,000 $m^3$, assuming a porosity of 20 to 40%. If the density of liquid $CO_2$ is 0.77 $t/m^3$, the injectable $CO_2$ is calculated to be 240 Mt-$CO_2$ at maximum. The amount injected by August 2018 was 0.2 Mt-$CO_2$ which is sufficiently smaller than the maximum injectable amount. Since the depth of the epicenters of the three micro-earthquakes was as deep as 7,400 - 7,700 m, it is unlikely that these three micro-earthquakes were caused by $CO_2$ injection, but here we treat them as induced earthquakes.

The total induced earthquake energy is seen in Table 1 to be 10% or less of the water injection energy for all the studied sites. However, the ratio of total induced earthquake energy to water injection energy varied greatly from 0.0001% to 6.4% by site.

## 3. DENSITY OF NATURAL FRACTURES

The magnitude of an induced earthquake is considered to be determined by the conditions of hydraulic fracturing and underground structures. Here we focus on natural fracture density within an underground structure. The natural fracture density of the six power generation test sites examined in this paper were obtained from prior studies in the literature.

### 3.1 Hijiori

Cores totaling 9.5 m in length were taken from well HDR-3 at the Hijiori site, and 229 fractures with a width of 1 mm or less were observed (Kitani and Tezuka, 2002). Therefore the natural fracture density in this rock was 24 /m.

### 3.2 Ogachi

Six cores were collected at depths between 730 and 1154 m from well OGC-3 at the Ogachi site. We focus on two cores obtained at depths 975 – 1154 m near the well bottom (Itoh, 2001). The total length of these cores was 4.1 m and the number of fractures was 15, yielding a natural fracture density of 3.7 /m.

### 3.3 Newberry

From the Borehole Tele Viewer data of well 55-29 at the Newberry site, 351 cracks were observed between the depths of 1970 m and 2660 m (width 690 m), so the natural fracture density was 0.5 /m.

### 3.4 Soultz

The average natural fracture density of rock from well GPK-1 in Soultz was 3.2 /m (Baria et al., 2006), but the natural fracture density near the bottom of the well (4600-5100 m) was 0.6 /m (Dezayes et al., 2004). The latter value was adopted for this study.

### 3.5 Basel

The natural fracture density of rock below 3 km depth at this site was reported to be 0.3 /m (Ziegler et al., 2015).

### 3.6 Cooper Basin

Natural fracture density at the Cooper Basin site has been reported to be 0.2 /m to 0.1 /m (Nelson et al., 2007), and the average fracture density was taken as 0.15 /m.

Table 2 shows natural fracture density D, maximum magnitude $M_{max}$ of earthquake induced by hydraulic fracturing, and induced earthquake energy $E_{max}$ of the maximum magnitude for each of the sites.

**Table.2**

| Site | Natural Fracture Density D (/m) | Maximum Magnitude $M_{max}$ | Induced Earthquake Energy $E_{max}$ (GJ) |
|---|---|---|---|
| Hijiori | 24 | 0.3 | 0.0002 |
| Ogachi | 3.7 | 2.0 | 0.06 |
| Newberry | 0.5 | 2.6 | 0.5 |
| Soultz | 0.6 | 2.6 | 0.5 |
| Basel | 0.3 | 3.4 | 7.9 |
| Cooper Basin | 0.15 | 3.7 | 22.4 |

Figure 2 shows the relationship between maximum magnitude and the logarithm of natural fracture density from Table 2. With good agreement, the maximum magnitude was found to be negatively correlated to the logarithm of the natural fracture density.

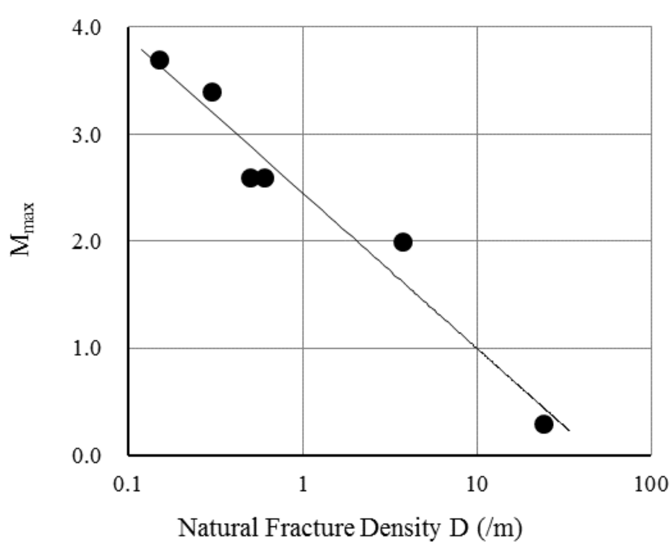


**Figure 2: Maximum magnitude and natural fracture density.**

## 4. INTERVAL DISTRIBUTION OF NATURAL FRACTURE

Since the maximum earthquake magnitude shows a negative proportional relationship with the logarithm of the natural fracture density as shown in Figure 2, the horizontal axis can be replaced by Log (1/D).

Four of the examined sites (Newberry, Soultz, Basel, and Cooper Basin) have data on the magnitudes multiple induced earthquakes in addition to the maximum magnitude. Figure 3 shows 1) the relationship between induced earthquake energy $E_{max}$ (from Table 2) and Log(1/D), and 2) the relationship between total induced earthquake energy $E_{st}$ (from Table 1) and Log(1/D). It can be seen in Figure 3 that induced earthquake energy $E_{max}$ and total induced earthquake energy $E_{st}$ at the Basel and Cooper Basin sites are closer than those of the Soultz and Newberry sites.

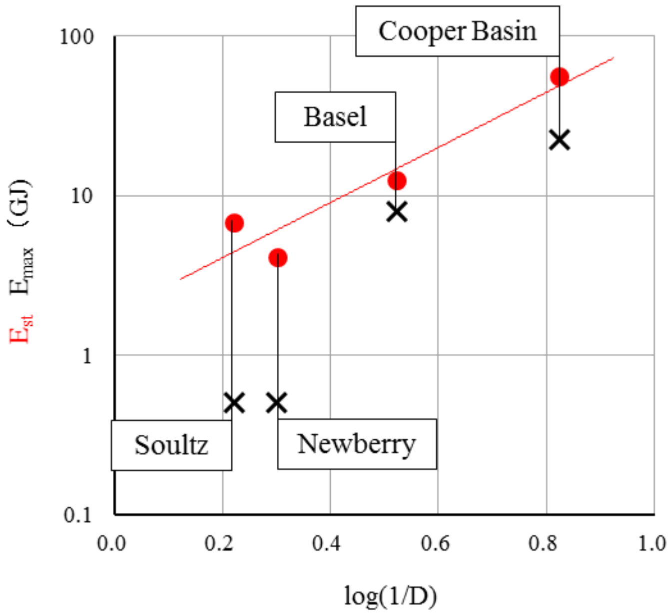


**Figure 3: Total induced earthquake energy $E_{st}$ and induced earthquake energy of maximum magnitude $E_{max}$.**

Table 3 shows the ratio of induced earthquake energy $E_{max}$ to total induced earthquake energy $E_{st}$ for these same four sites.

**Table 3**

| Site | $E_{max}$ (GJ) | $E_{st}$ (GJ) | $E_{max}$ /$E_{st}$ (%) |
|---|---|---|---|
| Newberry | 0.5 | 4.1 | 12 |
| Soultz | 0.5 | 6.8 | 7 |
| Basel | 7.9 | 12.5 | 63 |
| Cooper Basin | 22.4 | 55.9 | 40 |

We find that the maximum magnitude of an induced earthquake is strongly related to the natural fracture density, as shown in Figure 2. If intervals of natural fracture are equal, magnitudes of induced earthquakes are nearly equal, and the ratio of the maximum induced earthquake energy to the total induced earthquake energy is low. High values of this ratio, e.g. 40% and 63%, indicate that the interval variation of natural fractures is large.

## 5. EMPIRICAL FORMULA

Since the total induced earthquake energy $E_{st}$ was not only related to the water injection energy $E_i$ but also found to be very nearly proportional to Log (1/D) as shown in Figure 3, the following empirical formula is suggested.

$$E_{st} = 0.08 \text{ Log}(1/D - 0.1)E_i \quad (3)$$

Table 4 shows the results of applying formula (3) to the four sites (Newberry, Soultz, Basel, and Cooper Basin) where data on magnitudes of induced earthquakes other than maximum magnitude were disclosed.

**Table 4**

| Site | Observed $E_{st}$ (GJ) | Empirical formula $E_{st}$ (GJ) |
| --- | --- | --- |
| Newberry | 4.1 | 7.7 |
| Soultz | 6.8 | 4.7 |
| Basel | 12.5 | 11.7 |
| Cooper Basin | 55.9 | 57.5 |

Values calculated using the empirical formula are roughly in agreement with observed values. It was found that total induced earthquake energy can be formulated using water injection energy and natural fracture density.

It is necessary to consider factors other than the natural fracture density to better predict the observed energy values from the empirical formula. Among these factors are subsurface structure parameters such as opening widths of natural fractures, lengths of natural fractures, and rock strength.

Since only the data on maximum magnitude have been released for the Hijiori and Ogachi sites, the data from these sites were not used in the formulation of Equation (3).

## 6. CONCLUSION

We analyzed the magnitude of induced earthquakes caused by hydraulic fracturing from the viewpoint of energy balance. We investigated eight sites of hydraulic fracturing, wastewater injection, and CCS. We found that the total induced earthquake energy $E_{st}$ was less than 10% of water injection energy $E_i$ at all of these sites. However, it was found that the ratio of total induced earthquake energy $E_{st}$ to water injection energy $E_i$ varied greatly from 0.0001% to 6.4% depending on the site.

We clarified that the underground rock structure influences the magnitude of induced earthquakes. We showed that the maximum magnitude $M_{max}$ of an induced earthquake has a negative proportional relationship to the logarithm of natural fracture density D, and that the interval distribution of natural fracture affects the ratio of maximum induced earthquake energy $E_{max}$ to the total induced earthquake energy $E_{st}$. We also showed that total induced earthquake energy $E_{st}$ can be expressed as a function of water injection energy $E_i$ and natural fracture density D.

It is important to investigate the number and interval distribution of natural fractures by analysis of geological core samples and through Borehole Tele Viewer logging. This study found that clarifying the underground structure is effective for selecting potential locations for hot dry rock power generation and for reducing the incidence of induced earthquakes.

## REFERENCES

Baria, R., Jung, R., Tishner, T., Nicholls, J., Michelet, S., Sanjuan, B., Soma, N., Asanuma, H., Dyer, B. and Garnish, J.: Creation of an HDR Reservoir at 5000m Depth at the European HDR Project, Proc. 31st Workshop on Geothermal Reservoir Engineering, Stanford University. (2006).

Boroumand, N. and Eaton, D.: Comparing energy calculations: Hydraulic fracturing and microseismic monitoring. GeoConvention 2012: Vision, 14-18 May 2012, Calgary, Alberta, Canada.

Dezayes, C., Genter, A. and Gentier, S.: Fracture Network of the EGS Geothermal Reservoir at Soultz-sous-Foret, GRC Transactions Vol.28 213-218. (2004)

Dorbath, L., Cuenot, N., Genter, A. and Frogneux, M.: Seismic response of the fractured and faulted granite of Soultz-sous-Forets (France) to 5 km deep massive water injections. Geophys. J. Int. (2009).

Gutenberg, B. and Richter, C.F.: Magnitude and energy of earthquakes. Ann. Geofis., 9, 1-15. (1956).

Geothermal Data Repository, U.S Department of Energy, https://gdr.openei.org/submissions/271.

Geoscience Australia, Earthquake Database, http://www.ga.gov.au/earthquakes/searchQuake.do.

Häring, M.O., Schanz, U., Ladner, F. and Dyer, B.C.: Charcterisation of the Basel 1 enhanced geothermal system, Geothermics, 37, 469-495. (2008).

Itoh, H.: Estimation of Fracture Structure in Reservoir for Hot Dry Rock Geothermal Power (3) -Fracture Distribution and Characteristics Evaluated by Wellbore Wall Image Analysis-, Central Research Institute of Electric Power Industry U01004. (2001).

Japan CCS Co., Ltd., www.jccs-tomakomai-monitoring.com/JCCS/wp-content/uploads/2018/06/201806_ENG.pdf

Kaieda, H., Sasaki, S. and Wyborn, D.: Comparison of Characteristics of Micro-Earthquakes Observed During Hydraulic Stimulation Operations in Ogachi, Hijiori and Cooper Basin HDR Projects. Proc. World Geothermal Congress. (2010).

Kitani, S. and Tezuka, K.: Geologic Structure and Fracture System of HDR Reservoir on NEDO Hijiori Field in Yamagata Prefecture, Northeast Japan, J. Geothermal Research Society of Japan Vol. 24, 245-265. (2002).

Nelson, E. J., Chipperfield, S. T., Hillis, R. R., Gilbert, J. and McGowen, J.: Using geological information to optimize fracture stimulation practices in the Cooper Basin, Australia, Petroleum Geoscience Vol.13 3-16. (2007).

Petty, S., Nordin, Y., Glassley, W., Cladouhos, T. and Swyer, M.: Improving Geothermal Project Economics with Multi-Zone Stimulation: Results from the Newberry Volcano EGS Demonstration. Proc. 38th Workshop on Geothermal Reservoir Engineering, Stanford University. (2013).

Schoenball, M. and Kohl, T.: The Peculiar Shut-In Behavior of the Well GPK2 at Soultz-sous-Forets, GRC Transactions Vol.37. (2013).

Swiss Seismological Service (SED), Erdbebenkatalog, http://hitseddb.ethz.ch:8080/ecos09/query_sum.

Yamada, K., and Ishikawa, T.: Quantitative Analysis of Earthquake Energy Induced by Water Injection for Hot Dry Rock Power Generation, Proceedings 39th New Zealand Geothermal Workshop. (2017).

Ziegler, M., Valley, B. and Evans, K.: Characterisation of Natural Fractures and Fracture Zones of the Basel EGS Reservoir Inferred from Geophysical Logging of Basel-1 Well, Proceedings World Geothermal Congress. (2015).